J|A|C|S
ARTICLES
Published on Web 01/10/2002

Membrane Protein Topology Probed by ^{1}H Spin Diffusion from Lipids Using Solid-State NMR Spectroscopy

Daniel Huster, Xiaolan Yao, and Mei Hong*

Contribution from the Department of Chemistry, Iowa State University, Gilman Hall 0108, Ames, Iowa 50011

Received September 4, 2001. Revised Manuscript Received October 6, 2001

Abstract: We describe a two-dimensional solid-state NMR technique to investigate membrane protein topology under magic-angle spinning conditions. The experiment detects the rate of ^{1}H spin diffusion from the mobile lipids to the rigid protein. While spin diffusion within the rigid protein is fast, magnetization transfer in the mobile lipids is an inefficient and slow process. Qualitative analysis of ^{1}H spin-diffusion build-up curves from the lipid chain-end methyl groups to the protein allows the identification of membrane-embedded domains in the protein. Numerical simulations of spin-diffusion build-up curves yield the approximate insertion depth of protein segments in the membrane. The experiment is demonstrated on the selectively ^{13}C labeled colicin Ia channel domain, known to have a membrane-embedded domain, and on DNA/cationic lipid complexes where the DNA rods are bound to the membrane surface. The experiment is designed for X-nucleus detection, which could be ^{13}C or ^{15}N in the protein and ^{31}P for the DNA. Finally, we show that a qualitative distinction between membrane proteins with and without a membrane-embedded domain can be made even by using an unlabeled protein, by detection of lipid signals. This spin-diffusion experiment is simple to perform and requires no oriented bilayer preparations and only standard NMR hardware.

Introduction

The orientation topology of membrane-bound proteins is an important aspect of the overall structure that underlies the function of these essential molecules. For instance, for peptides and proteins that spontaneously bind and insert into bacterial membranes, knowledge of the locations of various amino acid residues in the protein relative to the lipid bilayer can shed light on the mechanism of membrane insertion. A number of techniques are available to probe the locations of protein segments with respect to the lipid bilayer. For example, site-specific spin labels combined with electron paramagnetic resonance spectroscopy have been used to monitor protein immersion in the membrane.[1,2] Fluorescence energy transfer from lipids to proteins[3] and site-selective photolabeling of transmembrane proteins[4] have also been shown to be useful. In high-resolution nuclear magnetic resonance (NMR) experiments, qualitative topology of peptides bound to micelles has been investigated by adding paramagnetic spin labels to the micelles.[5,6] Residues that exhibit a close proximity to the spin label are identified by resonance line broadening and chemical shift changes. This allows peptide segments in the micelle interior, surface, or the aqueous phase to be distinguished.[7−10] As compared to these techniques, solid-state NMR has the advantages that it requires no bulky extrinsic probes and makes use of lipid bilayers rather than detergent micelles to study membrane peptides and proteins. Particularly useful for elucidating membrane protein topology is the polarization-inversion-spin-exchange-at-the-magic-angle (PISEMA) experiment,[11] in which the tilt angles of helical peptides with respect to the bilayer normal are readily determined.[12,13] However, the PISEMA approach requires uniaxially aligned proteins in stacks of lipid bilayers. Such macroscopically oriented samples are difficult to make for large membrane proteins. More recently, paramagnetic O_2 has been used to probe the immersion depth of membrane proteins by monitoring the effect of pressurized O_2 on the relaxation rates and chemical shifts of ^{19}F spectra.[14,15]

* To whom correspondence should be addressed. E-mail: mhong@iastate.edu. Tel: (515) 294-3521. Fax: (515) 294-0105.

(1) Shin, Y.; Levinthal, C.; Levinthal, F.; Hubbell, W. L. *Science* **1993**, *259*, 960−963.
(2) Altenbach, C.; Greenhalgh, D. A.; Khorana, H. G.; Hubbell, W. L. *Proc. Natl. Acad. Sci. U.S.A.* **1994**, *91*, 1667−1671.
(3) Lakey, J. H.; Duche, D.; Gonzalez-Manas, J.; Baty, D.; Pattus, F. *J. Mol. Biol.* **1993**, *230*, 1055−1067.
(4) Ogawa, Y.; Hahn, W.; Garnier, P.; Higashi, N.; Massotte, D.; Metz-Boutigue, M.; Rousseau, B.; Sunamoto, J.; Ourisson, G.; Nakatani, Y. *Angew. Chem., Int. Ed.* **2001**, *40*, 944−946.
(5) Papavoine, C. H.; Konings, R. N.; Hilbers, C. W.; vandeVen, F. J. *Biochemistry* **1994**, *33*, 12990−12997.
(6) O'Neil, J. D.; Sykes, B. D. *Biochemistry* **1989**, *28*, 699−707.
(7) Schibli, D. J.; Hwang, P. M.; Vogel, H. J. *Biochemistry* **1999**, *38*, 16749−16755.
(8) Losonczi, J. A.; Olejniczak, E. T.; Betz, S. F.; Harlan, J. E.; Mack, J.; SW., S. W. F. *Biochemistry* **2000**, *39*, 11024−11033.
(9) Chupin, V.; Killian, J. A.; Breg, J.; Jongh, H. H. d.; Boelens, R.; Kaptein, R.; Kruijff, B. d. *Biochemistry* **1995**, *34*, 11617−11624.
(10) Jarvet, J.; Zdunek, J.; Damberg, P.; Graslund, A. *Biochemistry* **1997**, *36*, 8153−8163.
(11) Wu, C. H.; Ramamoorthy, A.; Opella, S. J. *J. Magn. Reson., Ser. A* **1994**, *109*, 270−272.
(12) Marassi, F.; Opella, S. *Curr. Opin. Struct. Biol.* **1998**, *8*, 640−648.
(13) Fu, R.; Cross, T. A. *Annu. Rev. Biophys. Biomol. Struct.* **1999**, *28*, 235−268.
(14) Prosser, R. S.; Luchette, P. A.; Westerman, P. W. *Proc. Natl. Acad. Sci. U.S.A.* **2000**, *97*, 9967−9971.
(15) Prosser, R. S.; Luchette, P. A.; Westerman, P. W.; Rozek, A.; Hancock, R. E. W. *Biophys. J.* **2001**, *80*, 1406−1416.

10.1021/ja017001r CCC: $22.00

This method requires ^{19}F-labeled proteins, which are relatively difficult to obtain as compared to ^{13}C and ^{15}N labeled proteins.

Proton spin diffusion represents an alternative strategy to study membrane protein topology of nonoriented bilayer samples. In the spin-diffusion approach, magnetization from well-defined sources is selected based on the mobility or other spin properties and is allowed to transfer to the desired targets in the protein. The magnetization transfer is facilitated by dipolar couplings between two protons. Since the dipolar coupling is distance dependent, the rate of transfer is determined by the proximity of the sink spins to the source spins; thus it yields the spatial distribution of protein segments in the lipid membrane. The liquid-crystalline nature of the lipid bilayer can be accommodated by solid-state NMR, and high-resolution ^{1}H and ^{13}C spectra can be obtained by magic angle spinning (MAS).[16]

Recently, a ^{1}H spin-diffusion experiment utilizing water as the magnetization source has been demonstrated and applied to the membrane-bound colicin E1 channel domain.[17] In this experiment, the membrane sample was frozen to the gel phase, and a ^{1}H T_2 filter was used to select the mobile ^{1}H spins in the system. Because of the rigidity of both the lipids and the protein, the ^{1}H signals from these molecules were suppressed by the T_2 filter. However, water molecules remain mobile at the temperatures used and retain their magnetization. These water protons thus serve as the source of the spin diffusion into the magnetization-depleted protein and lipid molecules. The experiment showed that a significant fraction of the colicin E1 channel domain resides close to the water molecules. In other words, the protein has a sizable surface-bound fraction.

This water-initiated ^{1}H spin-diffusion experiment was limited to temperatures below the gel-to-liquid-crystalline phase transition temperature of the lipids to keep the lipids immobile. The requirement of low-temperature MAS restricts the applicability of the experiment. Moreover, since the water molecules mostly reside on the surface of the lipid bilayer, the experiment cannot sensitively detect the residues embedded in the hydrophobic core of the lipid bilayer.

In this paper, we describe a complementary ^{1}H spin-diffusion technique that initiates the magnetization transfer from the lipid protons, specifically the methyl protons at the center of the bilayer. We show that this technique detects membrane-embedded segments in a protein sensitively, even at ambient temperatures. The principle of this approach is illustrated in Figure 1. The experiment exploits the large difference in the magnetization transfer rates between a rigid macromolecule and the mobile lipids at ambient temperature. A protein with transmembrane domains provides rigid segments close to the center of the liquid-crystalline bilayer; thus spin diffusion from the lipid methyl protons to the protein protons is rapid (pathway a). In contrast, for a protein with only surface-bound segments, the methyl ^{1}H magnetization must first diffuse through the lipid acyl chains before reaching the protein. Since spin diffusion in the lipids is extremely slow as a result of motionally averaged ^{1}H−^{1}H dipolar couplings (pathway b), the surface-bound protein receives little ^{1}H magnetization from the methyl protons in the same time period. The distribution of methyl groups in fluid bilayers is relatively narrow; joint refinement of X-ray and neutron diffraction data showed a width of about 6 Å at half-height along the bilayer normal,[18] combining both leaflets. Thus, methyl protons provide well-defined source magnetization in the bilayer center, from which one may derive the maximum depth of insertion of the protein.

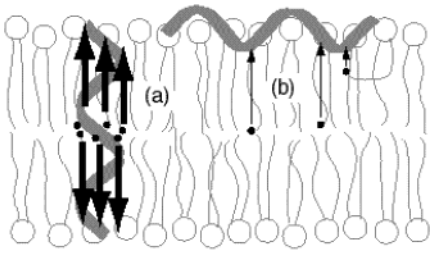

Figure 1. Illustration of a lipid bilayer with a transmembrane (a) and an interface-bound α-helix (b). (a) Magnetization from the lipid chain terminus is transferred to the protein, where spin diffusion is extremely fast due to the strong ^{1}H−^{1}H dipolar couplings. This efficient pathway is indicated by thick arrows. (b) Magnetization from the chain terminus is transferred through the lipid acyl chains for a large distance before reaching the protein. This is a slow process, indicated by thin arrows.

We demonstrate this new approach by comparing the spin-diffusion behavior of a protein, colicin Ia channel domain, which has a membrane-embedded domain, to the spin diffusion of membrane-bound DNA, which has only surface-residing domains. For colicin, two possible topological models have been proposed to describe its closed-channel state. In the "umbrella model", two hydrophobic helices, C8 and C9, are inserted in a transmembrane fashion, parallel to the bilayer normal, while eight amphipathic helices are located at the lipid−water interface.[19] In comparison, the "penknife model" postulates that all helices are oriented approximately perpendicular to the bilayer normal, with the C8 and C9 helices exposed to the hydrophobic interior but tugged close to the rest of the protein at the membrane−water interface.[3] A comparison of the experimental spin-diffusion build-up curves for colicin and DNA strongly supports the umbrella model for colicin. While we first applied this ^{1}H spin-diffusion technique to ^{13}C-labeled colicin, we later show that it can also be used on unlabeled samples to obtain membrane protein topology, through indirect detection of the lipid signals.

Experimental Procedures

Materials. 1-Palmitoyl-d_{31}-2-oleoyl-*sn*-glycero-3-phosphocholine (POPC-d_{31}), 1-palmitoyl-2-oleoyl-*sn*-glycero-3-phosphoglycerol (POPG), and 1,2-dioleoyl-3-trimethylammonium-propane (DOTAP) were purchased from Avanti Polar Lipids, Inc. (Alabaster, AL) and used without further purification. $^{15}NH_4Cl$, ^{15}N-Glu, and [2-^{13}C] glycerol were purchased from Cambridge Isotope Laboratories (Andover, MA). Unlabeled amino acids and deoxyribonucleic acid (DNA) from calf thymus were purchased from Sigma (St. Louis, MO).

Protein Expression. The colicin Ia channel domain was labeled selectively and extensively in ^{13}C and uniformly in ^{15}N following the TEASE (10 amino acid selective and extensive labeling) labeling protocol published earlier.[20] The protein was expressed from pKSJ120-containing *E. coli* BL21 (DE3). Cells were grown overnight at 37 °C in 100 mL of a modified M9 medium containing, per liter, 1 g of NH_4Cl, 4 g of glycerol, 3 g of KH_2PO_4, 6 g of Na_2HPO_4, 0.5 g of NaCl, 15

(16) Forbes, J.; Husted, C.; Oldfield, E. *J. Am. Chem. Soc.* **1988**, *110*, 1059−1065.
(17) Kumashiro, K. K.; Schmidt-Rohr, K.; Murphy, O. J.; Ouellette, K. L.; Cramer, W. A.; Thompson, L. K. *J. Am. Chem. Soc.* **1998**, *120*, 5043−5051.
(18) Wiener, M. C.; White, S. H. *Biophys. J.* **1992**, *61*, 434−447.
(19) Parker, M. W.; Postma, J. P. M.; Pattus, F.; Tucker, A. D.; Tsernoglou, D. *J. Mol. Biol.* **1992**, *224*, 639−657.
(20) Hong, M.; Jakes, K. *J. Biomol. NMR* **1999**, *14*, 71−74.

mg of $CaCl_2$, 1 mM $MgSO_4$, the unlabeled amino acids Asp, Asn, Arg, Gln, Ile, Lys, Met, Pro, Thr, and Glu at 150 μg/mL each, and 100 μg/mL ampicillin. The cells were pelleted and resuspended in 10 mL of the same medium, but containing 1.5 g of $^{15}NH_4Cl$, [2-^{13}C] glycerol, and 150 μg/mL ^{15}N-Glu instead of unlabeled Glu. Those cells were used to inoculate 1 L of the stable isotope-containing medium. The culture was grown at 37 °C to $OD_{660} = 0.4$ and then induced with 1 mM IPTG. Cells were harvested after 3 h of induction at 37 °C. The soluble His-tagged colicin Ia channel domain was purified on His-Bind metal chelation resin (Novagen, Madison, WI) as specified in the Novagen pET System Manual, except that the wash step was performed at 40 mM imidazole. The yield of the pure soluble protein was approximately 40 mg from 1 L of culture. Purified protein eluted from the His-Bind resin in 1 M imidazole buffer was dialyzed extensively against distilled water and lyophilized.

NMR Sample Preparation. The protocol for reconstituting the colicin Ia channel domain into phospholipid membranes was described recently.[21] Briefly, we prepared unilamellar POPC-d_{31}/POPG vesicles at a molar ratio of 3:1. This involved mixing the lipids in chloroform, lyophilizing the mixture, rehydrating it in a citrate buffer at pH 4.8, vortexing, and freeze-thawing. The resulting lipid suspension was then extruded across polycarbonate filter membranes with a pore size of 100 nm to obtain large unilamellar vesicles. Aliquots of the extruded lipid vesicles were combined with the appropriate amount of the colicin solution to reach a final protein:lipid molar ratio of 1:100. The protein−lipid mixture was ultracentrifuged at 150 000*g* for 2 h. This yielded 95% reconstitution of the protein into the lipids, as indicated by a photometric analysis. Since the membrane pellet typically contained about 80 wt % water, which is too wet for solid-state NMR experiments, we lyophilized the pellet and rehydrated it to a final water level of 30 wt % relative to the total sample weight. The membrane-bound colicin sample contained about 8 mg of protein and 24 mg of lipid.

For the DNA/DOTAP sample, 150 mg of DOTAP powder was dispersed in aqueous buffer (10 mM Hepes, pH 7.4). A total of 66 mg of DNA was dissolved in the same buffer, and aliquots of DNA solution were added to the DOTAP vesicles to achieve an isoelectric charge ratio between the positive DOTAP choline and the negative DNA phosphates. The mixtures were equilibrated by intensive vortexing and 10 freeze−thaw cycles.[22] The preparations were ultracentrifuged at 16 000*g*, and the pellet was transferred into a 7 mm MAS rotor and sealed.

NMR Spectroscopy. All NMR experiments were carried out on a Bruker DSX-400 spectrometer (Karlsruhe, Germany) operating at a resonance frequency of 400.49 MHz for ^{1}H, 162.12 MHz for ^{31}P, and 100.72 MHz for ^{13}C. A triple-resonance MAS probe with a 4 mm spinning module and a double-resonance 7 mm MAS probe were used. The ^{1}H radio frequency (rf) field strength for heteronuclear two-pulse phase modulation (TPPM) decoupling[23] was about 50 and 62.5 kHz for the DNA and colicin samples, respectively. Typical ^{1}H and ^{13}C/^{31}P 90° pulse lengths were 4 and 5 μs, respectively. Cross polarization (CP) was achieved with spin-lock fields of about 50 kHz. The CP contact time was 0.5 ms for the colicin sample and 0.7 ms for the DOTAP/DNA sample. On the ^{1}H channel, Lee-Goldburg (LG) spin lock was used to suppress ^{1}H spin diffusion during CP. This requires that the effective ^{1}H field strength ($\omega_{eff,H}$) matches the X-channel spin-lock field strength, with an applied ^{1}H rf field strength of $\omega_{eff,H}$ sin(54.7°) and a ^{1}H frequency offset of $\omega_{eff,H}$ cos(54.7°).

^{1}H MAS nuclear Overhauser enhancement spectroscopy (NOESY) experiments were conducted at a spinning speed of 6 kHz using the standard solution NMR pulse sequence.[24] The 90° pulse length was 4.5 μs, and the mixing times were varied between 1 and 500 ms. Cross-peak volumes were integrated using xwinnmr software (Bruker Analytische Messtechnik, Rheinstetten, Germany). The relaxation matrix for the lipid protons was calculated as described previously.[25]

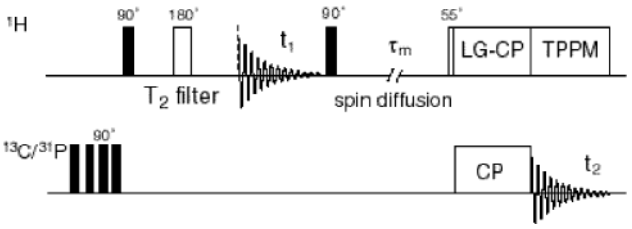

Figure 2. Pulse sequence for the 2-D MAS spin-diffusion experiment with ^{13}C or ^{31}P detection. LG-CP: Lee-Goldburg cross-polarization, TPPM: two-pulse phase modulation decoupling.

2-D ^{1}H spin-diffusion experiments were carried out using mixing times between 2 ms and 2.209 s. Typical spinning speeds were 4.5 kHz for the 7 mm rotor and 7 kHz for the 4 mm rotor. Spinning speeds were regulated to ±2 Hz by a pneumatic control unit. A T_2 filter time of 2 ms was applied to dephase the ^{1}H magnetization of the rigid colicin and DNA molecules, but retaining sufficient lipid ^{1}H magnetization. In the indirect dimension, between 96 and 136 data points were collected with a dwell time of one or two rotor periods. This yielded a total ^{1}H evolution time of approximately 18 ms, which is suitable for the relatively sharp ^{1}H lines of the lipids. The States detection method was used to obtain pure-absorptive spectra. The 2-D time data were zero-filled and Fourier transformed to yield a 2-D matrix of 256 × 1024 data points. A recycle delay of 2−3 s was used in the experiments. All measurements were carried out at room temperature ($T = 293 \pm 1$ K).

Spin-Diffusion Pulse Sequence. The pulse sequence for the 2-D ^{1}H spin-diffusion experiment with X-nucleus detection is shown in Figure 2. In the beginning, four 90° pulses on the X-channel destroy residual X-magnetization. After an initial 90° pulse on the ^{1}H channel, ^{1}H magnetization from mobile lipid segments is selected by a T_2 filter, while the ^{1}H signals of the more rigid protein or DNA relax due to the strong ^{1}H−^{1}H dipolar couplings. The 180° pulse in the middle of the T_2 filter refocuses the isotropic chemical shift evolution and B_0 field inhomogeneity. Next, the lipid ^{1}H magnetization evolves under the isotropic chemical shift interaction for the t_1 period. A ^{1}H 90° pulse then stores the magnetization along the *z*-axis and allows it to exchange via spin diffusion for a mixing period, τ_m. After the mixing time, the ^{1}H magnetization is flipped to the LG effective field direction by a magic-angle pulse of 54.7° and locked. Simultaneous spin-lock on the X-channel with equal field strengths transfers the ^{1}H magnetization to X-spins, which is then detected during t_2. Since a short contact time of 0.5 ms was used for LG-CP for the colicin sample, the ^{13}C signals of the mobile lipids are mostly suppressed in the spectrum.

Data Analysis. For quantitative analysis of 2-D spin-diffusion spectra, ^{1}H cross sections were extracted from the 2-D spectra at the desired ^{13}C or ^{31}P frequency. Peak intensities were recorded with respect to a reference spectrum, which corresponds to a mixing time of 100 ms for the colicin sample and 400 ms for the DNA sample. Peak intensities were plotted as a function of $\sqrt{\tau_m}$ and corrected for T_1 relaxation during the mixing time by multiplication with $\exp(\tau_m/T_1)$. ^{1}H spin−lattice relaxation times of lipid signals were measured using the standard inversion recovery sequence. Error bars in Figures 5, 6, 8, and 9 represent the noise level at the respective signals in the 2-D spectra.

Simulations. The spin-diffusion build-up curves were simulated as a function of mixing time using a one-dimensional lattice model.[17,26] In this model, each spin passes a fraction of its magnetization to its neighbors and in turn receives the same fraction of their magnetization

(21) Huster, D.; Xiao, L. S.; Hong, M. *Biochemistry* **2001**, *40*, 7662−7674.
(22) Mayer, L. D.; Hope, M. J.; Cullis, P. R.; Janoff, A. S. *Biochim. Biophys. Acta* **1985**, *817*, 193−196.
(23) Bennett, A. E.; Rienstra, C. M.; Auger, M.; Lakshmi, K. V.; Griffin, R. G. *J. Chem. Phys.* **1995**, *103*, 6951−6958.
(24) Jeener, J.; Meier, B. H.; Bachmann, P.; Ernst, R. R. *J. Chem. Phys.* **1979**, *71*, 4546−4554.
(25) Huster, D.; Arnold, K.; Gawrisch, K. *J. Phys. Chem.* **1999**, *103*, 243−251.
(26) Schmidt-Rohr, K.; Spiess, H. W. *Multidimensional Solid-State NMR and Polymers*, 1st ed.; Academic Press: San Diego, 1994.

according to the discrete diffusion equation:

$$\frac{\Delta M_i}{\Delta t} = -2\Omega M_i + \Omega M_{i+1} + \Omega M_{i-1} \quad (1)$$

The rate of magnetization transfer, $\Omega = D/a^2$, depends on the spacing between spins, a, and the diffusion coefficient, D. The transfer rate is related to the dipolar coupling between the ^{1}H spins. In rigid organic solids such as polymers, a diffusion coefficient of 0.8 nm^2/ms was measured.[27] This corresponds to a transfer rate, or dipolar coupling, of about 20 kHz between two protons 2 Å apart. In contrast, the diffusion coefficients for lipid acyl chains, membrane proteins, and DNA generally differ from that of the rigid solid due to restricted motions. For example, the motionally averaged ^{1}H−^{1}H coupling for a pair of lipid vicinal protons 2.4 Å apart near the center of the bilayer is only about 400 Hz, estimated from the ^{2}H quadrupolar couplings. With a proton spacing of 2 Å, the resulting diffusion coefficient is about 0.016 nm^2/ms. This is in rough agreement with the value of 0.012 nm^2/ms used in our simulations and also matches the DNA data shown below. For spin diffusion in colicin, a ^{1}H−^{1}H order parameter of 0.7 can be estimated from previous experiments,[21] which corresponds to an average dipolar coupling of about 6 kHz between vicinal protons. This yields a diffusion coefficient of about 0.25 nm^2/ms, which agrees well with the empirical value of 0.3 nm^2/ms used in the simulations. As compared to magnetization transfer in the lipids and in the protein or DNA, the interfacial transfer rate is much slower, due to the fast uniaxial rotation and lateral diffusion of the lipids in the liquid-crystalline phase. With the same proton spacing of 2 Å, the optimized diffusion coefficient for the lipid−protein transfer is 0.0025 nm^2/ms, which corresponds to a transfer rate of 60 Hz. The spin-diffusion coefficient for the lipid−DNA interfacial transfer is even smaller at the same proton spacing. This may result from the lower ^{1}H density in DNA, especially near the phosphate groups.

The use of a 1-D lattice model for ^{1}H spin diffusion in colicin, which potentially has a complex three-dimensional structure, is justified by the following consideration. The ^{1}H−^{1}H dipolar couplings of the lipids are so much weaker than those of the protein that magnetization, once reaching the protein, transfers rapidly along the polypeptide chain. As long as the protein is loosely folded, the magnetization transfer may be considered as along an extended one-dimensional rod. Alternate pathways through the mobile lipids are highly inefficient due to their weak dipolar couplings. The approximation of a loosely folded colicin is valid, since previous fluorescence experiments on the colicin E1 channel domain, a homologous protein, suggested that the protein forms an extended helical array on the surface of the membrane.[28] Using this linear rod model, the total chain length of the colicin Ia channel domain would be about 150 Å. However, simulations show that the spin-diffusion build-up curves are largely independent of this length, since spin diffusion is primarily determined by the rate-limiting steps of magnetization transfer across the lipid−protein interface. Because of this large contrast between the protein and lipid spin-diffusion rates, the different geometries of the colicin Ia channel domain in the umbrella model and the penknife model also do not influence the spin-diffusion build-up curves. Only the smallest separation between the lipid methyl groups and the protein, which differs between the two models, influences the build-up curves.

In addition to the various diffusion coefficients and the ^{1}H spacing, the simulations use well-established values of lipid bilayer dimensions along the bilayer normal. At 22 °C, POPC bilayers have an acyl chain length of about 14.6 Å, a distance from the headgroup to the bilayer center of about 23.2 Å, and a water layer thickness of about 19 Å.[29]

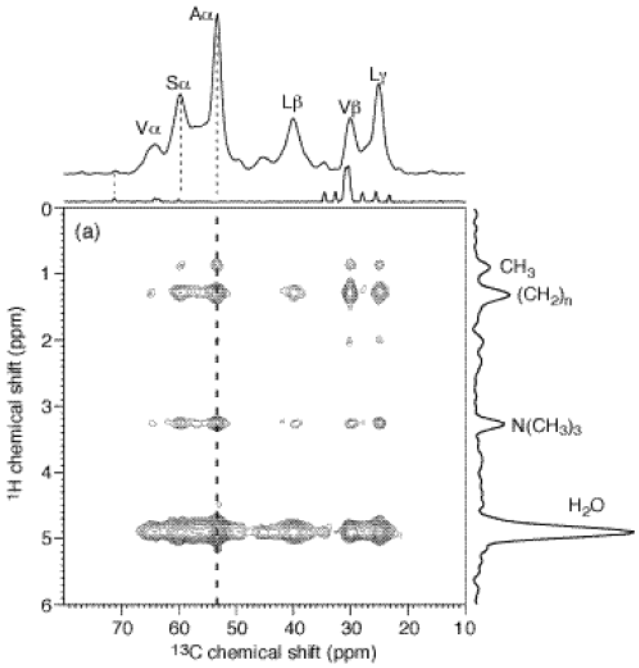

Figure 3. 2-D ^{13}C-detected ^{1}H spin-diffusion spectrum of the membrane-bound colicin Ia channel domain, with a mixing time of 100 ms. A T_2 filter time of 2 ms, a relaxation delay of 3 s, and a spinning speed of 7 kHz were used. The 128 t_1 increments were acquired with 96 transients per increment. Above the 2-D spectrum, the ^{13}C projection of the protein (top) is shown, where the assignment is based on previous work.[21] Below the projection is a ^{13}C CP spectrum of pure POPC/POPG lipids under the same experimental conditions. The lipid ^{13}C signal is negligible as compared to that of the protein. On the right-hand side, a ^{1}H cross section from the Ala Cα peak (53.2 ppm, dotted line in 2-D) is shown.

The diameter of the DNA rods between the opposing bilayers is 20 Å, based on diffraction studies on the same model system.[30]

The simulated magnetization build-up curves for sink spins at varying distances from the source magnetization are summed to yield a single build-up curve and compared with the experimental data. The summation is necessary since the NMR experiments here detect the average signals of each amino acid type rather than a single residue. Each type of residues exists in multiple copies in the protein and thus must be located at various places relative to the membrane. Importantly, this lack of single-site resolution does not affect the determination of the presence or absence of transmembrane domains and their maximum depths of insertion, since the large ^{1}H−^{1}H couplings within the rigid protein equilibrate the ^{1}H magnetization rapidly. Rather, the orientation information is extracted from the minimum distance between the protein and the center of the bilayer; the larger this distance is, the slower the spin diffusion.

Results

^{13}C-Detected ^{1}H Spin Diffusion from Lipid into Colicin. Figure 3 shows a representative 2-D ^{13}C-detected ^{1}H spin-diffusion spectrum of the membrane-bound colicin Ia channel domain, obtained with a mixing time of 100 ms. The source and sink of spin diffusion are readily distinguished in the 2-D spectrum; the ^{13}C chemical shifts of the peaks mark the sinks of spin diffusion in the protein, while the ^{1}H chemical shifts indicate the sources of the magnetization. A projection along the ^{13}C (ω_2) dimension is shown, where partial amino acid type assignment[31] is made on the basis of the TEASE ^{13}C-labeling pattern and previous 2-D correlation experiments.[20,32] In the side

(27) Clauss, J.; Schmidt-Rohr, K.; Spiess, H. W. *Acta Polym.* **1993**, *44*, 1−17.
(28) Lindeberg, M.; Zakharov, S. D.; Cramer, W. A. *J. Mol. Biol.* **2000**, *295*, 679−692.
(29) Pabst, G.; Rappolt, M.; Amenitsch, H.; Laggner, P. *Phys. Rev. E* **2000**, *62*, 4000−4009.
(30) Salditt, T.; Koltover, I.; Radler, J. O.; Safinya, C. R. *Phys. Rev. Lett.* **1997**, *79*, 2582−2585.

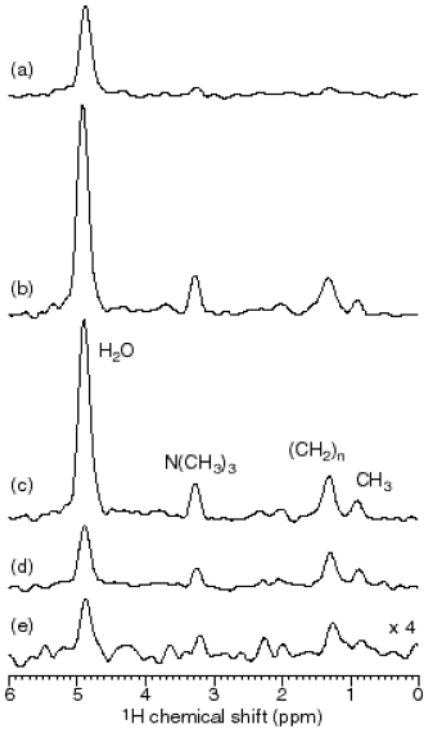

Figure 4. 1-D ^{1}H cross sections from the Ala Cα peak in various 2-D spectra of the membrane-bound colicin Ia channel domain. (a) $\tau_m = 2$ ms (224 scans per t_1 increment); (b) $\tau_m = 36$ ms (96 scans per t_1 increment); (c) $\tau_m = 100$ ms (96 scans per t_1 increment); (d) $\tau_m = 400$ ms (128 scans per t_1 increment); (e) $\tau_m = 900$ ms (256 scans per t_1 increment). Data are plotted to scale with respect to spectrum c.

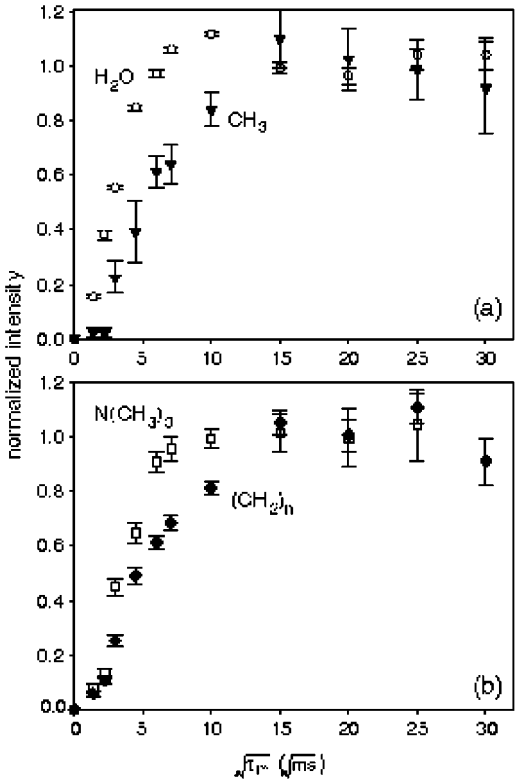

Figure 5. Spin-diffusion build-up curves as a function of mixing time for the Ala Cα signal in the colicin Ia channel domain. The magnetization sources are (a) H_2O (open circles) and CH_3 (filled triangles). (b) $N(CH_3)_3$ (open squares) and $(CH_2)_n$ (filled diamonds). Data were corrected for ^{1}H T_1 relaxation. Error bars represent the noise level of the ^{1}H peaks in the 2-D spectra.

chains, only Val β and Leu β and γ carbons are labeled. In the backbone Cα region, resonances from eight types of amino acids (Ala, Gly, His, Ser, Phe, Trp, Tyr, and Val) are observed. The lipid ^{13}C intensities are negligible, as shown by a ^{13}C CP spectrum of POPC/POPG lipids, acquired with the same CP contact time as the protein. The suppression of the lipid signals is due to the fast molecular motions of the lipids and the short LG-CP for ^{1}H−^{13}C polarization transfer.

The mixing-time-dependent 2-D spin-diffusion spectra are best analyzed by extracting ^{1}H cross sections at a specific ^{13}C frequency. The ^{1}H peaks in each column indicate the origins of magnetization transfer. A cross section at the Ala ^{13}Cα isotropic shift (53.2 ppm) is shown on the right-hand side of the contour plot, where magnetization transfer originating from lipid CH_3, $(CH_2)_n$, $N(CH_3)_3$, and water can be distinguished.

Figure 4 shows the ^{1}H cross sections at the Ala ^{13}Cα peak (53.2 ppm) as a function of the spin-diffusion mixing time. At a short mixing time of 2 ms, all cross peaks are rather weak, indicating that lipid ^{1}H magnetization has not transferred much to the protein. As the mixing time increases, the peak intensities increase, and then decrease due to the dominance of ^{1}H T_1 relaxation. T_1-corrected spin-diffusion build-up curves for various ^{1}H peaks at the Ala Cα cross section are shown in Figure 5. Panel a compares the magnetization transfer from the water protons and from the lipid chain methyl protons. The water curve (open circles) rises very steeply and reaches a plateau after about 50 ms, indicating that the ^{1}H magnetization has equilibrated. In comparison, the spin-diffusion build-up from the chain methyl protons is much slower, reaching a plateau after about 225 ms.

The difference between spin diffusion from water and from acyl chain methyl groups is also manifested in the other proton sources. Figure 5b compares the spin-diffusion curves from the headgroup Hγ protons and from the methylene protons in the middle of the acyl chains. The magnetization transfer from the headgroup protons equilibrated after only 50 ms, while the methylene build-up curve has a smaller slope and reaches the plateau at about 225 ms.

To determine the presence or absence of protein residues at the bilayer center, we simulated the build-up curves for spin diffusion from the lipid chain methyl protons to the Ala residues in colicin. Figure 6a shows the simulations for two structural models. The solid line represents the best-fit simulation using a topology that includes a transmembrane domain, while the dashed line represents a topology without a transmembrane domain. In both models, magnetization transfer involves three stages, from the methyl protons along the lipid acyl chain, across the interface to the protein, and within the protein. For the rate-limiting interface transfer, an optimal diffusion coefficient of 0.0025 nm^2/ms is used. Within the more rigid protein, the faster spin diffusion is represented by a diffusion coefficient of 0.3 nm^2/ms.[27] The central parameter in the simulation is the separation between the chain-end methyl protons and the protein. For the transmembrane model, a small separation is used. We find that the simulated curve for a gap of 2 Å agrees well with the experimental data, indicating that colicin contains a membrane-embedded domain that inserts all the way to the core of the

(31) Huster, D.; Yao, X.; Jakes, K.; Hong, M. *Biochim. Biophys. Acta* **2002**, in press.
(32) Hong, M. *J. Magn. Reson.* **1999**, *139*, 389−401.

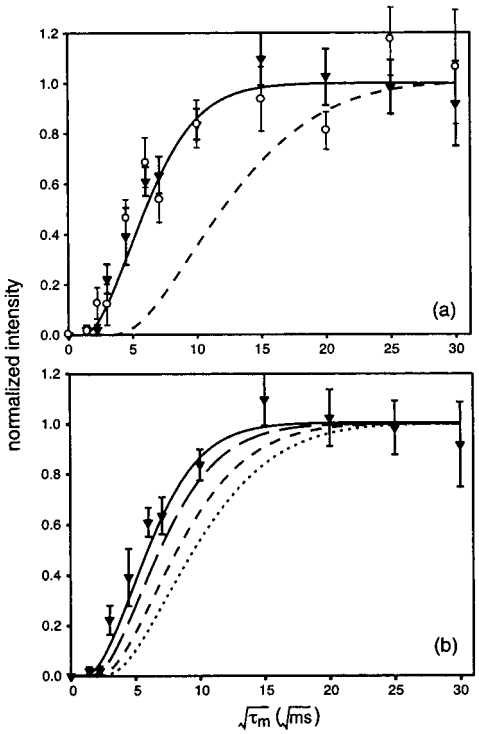

Figure 6. Simulations for the spin-diffusion build-up from lipid methyl protons to colicin. Filled triangles: Ala Cα intensities. Open circles: Ser Cα intensities. (a) Solid line: simulation using a gap of 2 Å between the methyl protons and the protein. Dotted line: simulation using a gap of 12 Å between the methyl protons and the protein. (b) Simulated spin-diffusion curves from methyl protons to the protein with varying gaps. Solid line: 2 Å. Long dashed line: 4 Å. Short dashed line: 6 Å. Dotted line: 8 Å.

hydrophobic bilayer. In contrast, if the colicin Ia channel domain resides only at the membrane−water interface, close to the glycerol backbone, then a gap of about 12 Å between the methyl protons and the protein is a reasonable estimate. The build-up curve for this distance (dashed line) is significantly shallower, since magnetization transfer along the lipid acyl chains is made inefficient by the weak $^1H-^1H$ dipolar couplings of the uniaxially mobile lipids. This reduced coupling is represented by a low diffusion coefficient of 0.012 nm^2/ms for the lipid chains. The 12 Å build-up curve deviates significantly from the observed data, indicating that colicin cannot be solely distributed at the membrane−water interface.

Since we detect the signals of all Ala Cα sites in the protein, the experimental methyl-to-Ala spin-diffusion build-up curve is an average among all Ala residues. This average nature indicates that the build-up curves for other residues must be similar. This is illustrated by the methyl-to-Ser (59 ppm) spin-diffusion curve in Figure 6a (open circles). It can be seen that the experimental intensities are well represented by the same simulation with a 2 Å gap between the acyl chain methyl protons and the protein.

We also simulated the build-up curves with varying distances between the methyl protons and the protein to further illustrate the degree of colicin insertion into the bilayer. As the distance increases, magnetization is transferred along the lipid chains over an increasing distance, thus resulting in slower build-up curves. Figure 6b shows the simulated spin-diffusion build-up curves for gaps of 4, 6, and 8 Å. As can be seen, the 6 and 8 Å curves deviate significantly from the experimental data, indicating that colicin reaches the bilayer center within 2−4 Å.

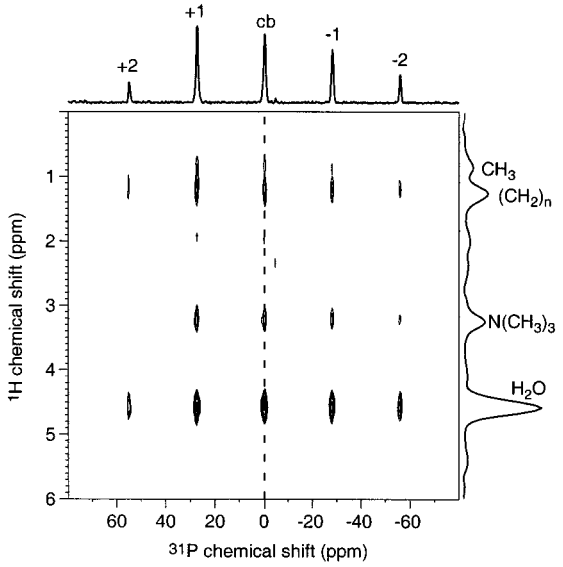

Figure 7. 2-D ^{31}P-detected ^1H spin-diffusion spectrum of a DNA/DOTAP mixture with a mixing time of 400 ms. A T_2 filter time of 2 ms, a relaxation delay of 3 s, and a spinning speed of 4.5 kHz were used. The 136 t_1 increments were acquired with 32 scans per increment. Above the 2-D spectrum is shown the projection along the ^{31}P dimension. The numbers refer to the spinning sideband order, cb: centerband. On the right-hand side, a ^1H column at the isotropic ^{31}P position (dotted line in 2-D plot) is shown.

^{31}P-Detected ^1H Spin Diffusion from Lipid into DNA. To demonstrate slow spin diffusion in the absence of a membrane-embedded macromolecule, we investigated ^1H magnetization transfer from cationic lipid membranes into surface-bound DNA molecules. These lipid/DNA complexes have received attention recently as nonviral gene transport vehicles into the cell.[33] X-ray diffraction revealed that addition of negatively charged DNA to positively charged lipid membranes results in densely packed stacks of cationic membranes with strands of DNA sandwiched between the surfaces of opposing bilayers.[34,35] No indication of DNA penetration into the bilayers was found. Thus, this lipid/DNA complex serves as a good model system for surface-bound macromolecules.

Figure 7 shows a representative 2-D $^1H-^{31}P$ correlated spin-diffusion spectrum of DOTAP/DNA complexes under 4.5 kHz of magic-angle spinning. The ^{31}P detection avoids interference from the DOTAP lipids, which do not contain a phosphate group. Spinning sidebands are observed in the direct dimension due to the large chemical shift anisotropy of DNA phosphate groups, which is 142 ppm (or 23 kHz at the ^{31}P Larmor frequency used here). The indirect dimension shows the ^1H spectrum of the source magnetization. Again, the most prominent spin-diffusion sources are water, lipid acyl chain $(CH_2)_n$, lipid headgroup $N(CH_3)_3$, and the lipid chain-end CH_3.

Figure 8 shows the build-up curve for spin diffusion from the chain terminal methyl protons to the DNA phosphates. The magnetization transfer does not reach a plateau even after a mixing time of 2209 ms. At 2209 ms, 97% of the ^1H magnetization is lost due to T_1 relaxation, thus prohibiting measurements at longer times. We scaled the last data point to

(33) Felgner, P. L. a. R. G. *Nature* **1991**, *349*, 351−352.
(34) Lasic, D. D.; Strey, H.; Stuart, M. C. A.; Podgornik, R.; Frederik, P. M. *J. Am. Chem. Soc.* **1997**, *119*, 832−833.
(35) Radler, J. O.; Koltover, I.; Salditt, T.; Safinya, C. R. *Science* **1997**, *275*, 810−814.

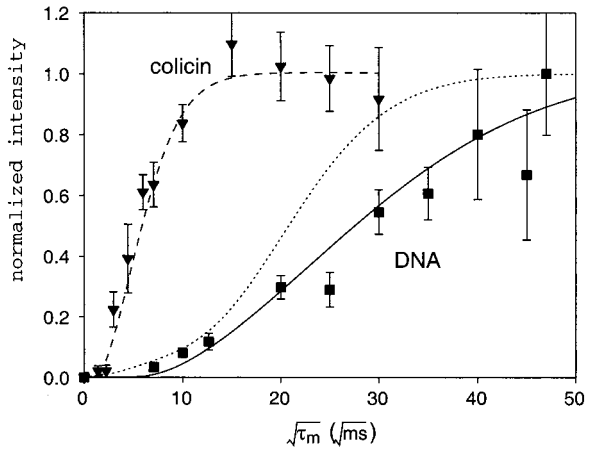

Figure 8. Comparison of spin-diffusion build-up from the lipid chain methyl protons to DNA (filled squares) and to colicin (filled triangles). Data points were corrected for T_1 relaxation. Lines represent simulated build-up curves. Solid line: methyl-to-DNA transfer with a distance of 20 Å. Dashed line: methyl-to-colicin transfer with a distance of 2 Å. The build-up curve for cross-relaxation between CH_3 and $N(CH_3)_3$ (dotted line), obtained from ^{1}H NOESY data[36] in the DNA/DOTAP sample, is also shown.

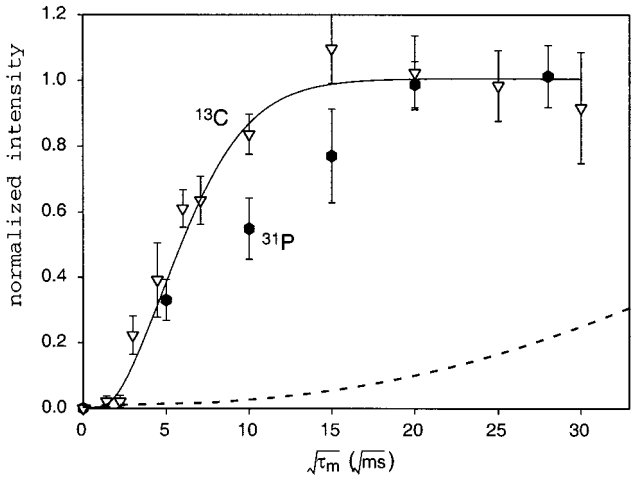

Figure 9. Spin-diffusion build-up from methyl to lipid headgroup ^{31}P (diamonds) in the presence of colicin. For comparison, the ^{13}C-detected methyl-to-Ala spin-diffusion curve (triangles and solid line) is shown. Also shown is the methyl-to-glycerol-3 ^{1}H spin-diffusion curve (dashed line) for a pure POPC/POPG membrane without any protein, obtained from previous ^{1}H NOESY data.[36]

1, although this may be a slight overestimate of the slope. Even with this maximal slope, it can be immediately recognized that spin diffusion into DNA is much slower than into colicin. For example, at 225 ms, the colicin build-up curve (dashed line) already reached its plateau (100%), while the DNA curve only reached about 15% of the final intensity. The dramatic difference between the two curves shows unambiguously that colicin contains a transmembrane domain and that this ^{1}H spin-diffusion method is extremely sensitive to the topologies of membrane-bound macromolecules.

Quantitative simulation of the DNA spin diffusion similarly involved three stages of magnetization transfer: from the methyl protons to the lipid headgroup, across the interface to DNA, and within DNA. The respective diffusion coefficients used are 0.012, 0.0003 (transfer rate = 7.5 Hz), and 0.1 nm^2/ms. X-ray diffraction studies gave a thickness of 23 and 20 Å for a single lipid leaflet and for the DNA, respectively.[30] In other words, the methyl ^{1}H magnetization is transferred slowly along the mobile acyl chains for 23 Å before reaching the rigid DNA. The simulated curve (solid line) using these parameters reproduces well the slow rise of the experimental data.

The slowness of magnetization transfer from the bilayer center to a surface-bound macromolecule is further demonstrated by spin diffusion from the methyl protons to the headgroup of DOTAP, in the presence of DNA. This intramembrane spin diffusion was investigated by a ^{1}H MAS NOESY experiment.[25,36] The experiment yielded a complete relaxation matrix for all lipid protons, from which we can plot the magnetization transfer curves between any pairs of protons. The methyl-to-headgroup magnetization exchange curve, shown as a dotted line in Figure 8, rises at a slightly steeper slope than the ^{31}P-detected methyl-to-DNA build-up curve. This is understandable, since the ^{31}P experiment requires one more step of magnetization transfer, from the headgroup into the DNA, than the ^{1}H NOESY experiment. This additional step is inefficient due to the weak dipolar couplings of the highly mobile DOTAP headgroup. Note that the ^{1}H NOESY approach is not suited for investigating the magnetization transfer from lipids into DNA because of the lack of resolved ^{1}H DNA signals.

The comparison between the ^{1}H NOESY data and the ^{31}P data suggests that the DNA spin diffusion may have just reached equilibrium after 2209 ms. Thus, a direct comparison between the build-up curves for colicin and for DNA is reasonable.

^{31}P-Detected ^{1}H Spin Diffusion from Lipid through Colicin. So far, the application of this lipid-initiated spin-diffusion method to membrane proteins relies on the detection of ^{13}C-labeled sites in the protein. While isotopic labeling increases the experimental sensitivity, it is expensive and may not be feasible for all membrane proteins. Thus, it is desirable to extend the spin-diffusion technique to unlabeled proteins to provide the same topological information. Since spin diffusion in transmembrane segments is so much faster than in the lipid chains, the methyl proton magnetization can "hijack" the rigid transmembrane segments to transfer to the bilayer surface efficiently. Moreover, a back transfer from the residues at the membrane surface to the lipid headgroup should be possible and may be detected through the lipid ^{31}P signal. This protein-assisted lipid-to-lipid magnetization transfer should be faster than magnetization transfer in the lipid chains in the absence of membrane-embedded protein domains.

Figure 9 shows the lipid ^{31}P-detected spin diffusion from the chain-end methyl protons. As expected, the magnetization build-up is fast, reaching a plateau at about 400 ms. As compared to the Ala Cα-detected build-up curve, the slope of the ^{31}P-detected curve is slightly lower, due to the additional back transfer from the protein to the lipids. Still, this ^{31}P-detected build-up curve is much steeper than the curve for the surface-bound DNA. Thus, from the ^{31}P-detected spectra, without requiring ^{13}C labeled proteins, we can conclude qualitatively that the membrane-bound colicin Ia channel domain possesses a deeply membrane-inserted domain.

Discussion

The orientational topology of membrane proteins is an important aspect of their three-dimensional structure. While

(36) Yau, W.; Gawrisch, K. *J. Am. Chem. Soc.* **2000**, *122*, 3971−3972.

membrane protein topology can sometimes be measured in detergent micelles using high-resolution NMR, the high curvature and the monolayer nature of micelles make them relatively poor membrane mimetics except for the smallest peptides. Further, spin labels may cause nonnegligible perturbation to the structure of the micelle−peptide complex. In comparison, precise topological information can be obtained without perturbing the membrane system by conducting ^{15}N solid-state NMR on macroscopically aligned bilayer samples.[37−43] However, this method requires well-oriented bilayers, which are increasingly difficult to prepare for larger membrane proteins.

The lipid-initiated ^{1}H spin-diffusion technique described here provides an alternative approach to obtain membrane protein topology information, without the need of macroscopic alignment. By exploiting the drastic difference between the ^{1}H magnetization transfer rates in lipids and in proteins,[44] we can obtain information about the presence or absence of transmembrane domains in the protein. This is manifested as the shortest distance between the methyl groups of the lipid chain ends and the protein. As compared to an earlier spin-diffusion experiment,[17] which transfers the water ^{1}H magnetization to the protein at low temperature, the current experiment can be conducted at room temperature. It also contains more structural information, since the 2-D spectrum resolves multiple magnetization sources, including lower lipid chain, upper lipid chain, lipid headgroup, and water. The experiment requires only a standard MAS probe and routine radio frequency powers and thus is easy to perform. With sufficient resolution, the analysis of the spin diffusion to the protein may also be site-specific.

Membrane Topology of the Colicin Ia Channel Domain. For the membrane-bound colicin Ia channel domain, spin diffusion from water and from the lipid headgroup is much faster than from the lipid chains (Figure 5). This indicates that more residues are located on the membrane surface than in the bilayer center. This relative population is obtained by considering the transfer rates across the protein−lipid interfaces and across the protein−water interface. The transfer from a mobile molecule to a rigid species is very slow, since the mobility of the magnetization source attenuates the ^{1}H−^{1}H dipolar couplings that drive spin diffusion. The mobilities of water, lipid headgroup, and acyl chain termini can be estimated from ^{2}H quadrupolar splittings, which are about 1−3 kHz for these deuterons.[45−47] These similar quadrupolar splittings indicate that the transfer rates across the water−protein, headgroup−protein, and chain end−protein interfaces are comparable. Thus, differences in the spin-diffusion rates from these ^{1}H sources must primarily result from different numbers of protein residues at the membrane−water interface versus those in the bilayer center. Figure 5 shows that the water and lipid headgroup build-up curves are similarly steep, while the methyl ^{1}H build-up curve is shallower. Thus, fewer residues in colicin are located in the center of the bilayer than at the membrane−water interface. The lipid methylene protons cannot be compared directly with the others, because their higher rigidity makes magnetization transfer more efficient.

In simulating the methyl-to-colicin spin-diffusion curve, the rate-limiting transfer across the interface is represented by a diffusion coefficient of 0.0025 nm^2/ms and a transfer rate of 62 Hz. These values are 20 times smaller than those used in simulating[17] the water−protein interface at low temperature. This is due to the higher mobility of the liquid-crystalline lipids. Once magnetization has reached the rigid protein, magnetization equilibrates rapidly. Thus, the exact length and shape of the colicin Ia channel domain does not affect the build-up curves. This was confirmed by the fact that simulations for protein chain lengths from 60 to 150 Å gave identical build-up curves.

The experimental methyl-to-colicin spin-diffusion data cannot be fit to a structural model that includes only surface-bound helices, but require a membrane-embedded domain in the protein. This is in broad agreement with both the umbrella model and the penknife model, since both models include a membrane-inserted domain comprising the hydrophobic helices C8 and C9. However, more detailed simulations using varying distances between the methyl groups and colicin indicate that the membrane-embedded domain of colicin cannot be separated from the bilayer center by more than 2−4 Å (Figure 6b). This close proximity favors the umbrella model. Thus, our data add to a growing number of recent studies that support the umbrella model for colicins. For example, ^{15}N NMR measurements of oriented colicin E1[41,42] showed a significant number of resolved signals in a region that corresponds to the transmembrane orientation. EPR and fluorescence studies also support the umbrella model.[1,48] However, our data do not rule out the possibility that the umbrella and penknife structures exist in a dynamic equilibrium, as suggested by conductivity measurements.[49]

The spin-diffusion simulations for colicin approximated the protein as a one-dimensional rod, based on the extended structure of the protein on the surface of the bilayer. This approximation does not restrict the current technique to this folding motif. For proteins with multiple transmembrane (TM) helices such as bacteriorhodopsin, the molecular shape is roughly a large-diameter cylinder containing all helices. Spin diffusion from the lipid methyl protons to the protein is then a function of the distance of the protein protons from the center of the bilayer. The build-up curves reflect the depth of residues from the center of the bilayer and are independent of the actual polypeptide chain folding into and out of the membrane and interhelical contacts. Spin diffusion in such predominantly TM proteins should be extremely fast.

Spin Diffusion in DOTAP/DNA Complexes. The DNA experiments demonstrate the spin-diffusion behavior in the absence of rigid TM segments. The DNA strands are sandwiched between opposing bilayers.[34,35] Negatively charged DNA only binds to the positively charged DOTAP surfaces without

(37) Opella, S. J.; Marassi, F. M.; Gesell, J. J.; Valente, A. P.; Kim, Y.; Oblatt-Montal, M.; Montal, M. *Nat. Struct. Biol.* **1999**, *6*, 374−379.
(38) Cross, T. A.; Opella, S. J. *Curr. Opin. Struct. Biol.* **1994**, *4*, 574−581.
(39) Glaubitz, C.; Burnett, I. J.; Gröbner, G.; Mason, A. J.; Watts, A. *J. Am. Chem. Soc.* **1999**, *121*, 5787−5794.
(40) Prosser, R. S.; Davis, J. H.; Dahlquist, F. W.; Lindorfer, M. A. *Biochemistry* **1991**, *30*, 4687−4696.
(41) Lambotte, S.; Jasperse, P.; Bechinger, B. *Biochemistry* **1998**, *37*, 16−22.
(42) Kim, Y.; Valentine, K.; Opella, S. J.; Schendel, S. L.; Cramer, W. A. *Protein Sci.* **1998**, *7*, 342−348.
(43) Marassi, F. M.; Opella, S. J. *J. Magn. Reson.* **2000**, *144*, 150−155.
(44) Takahashi, H.; Nakanishi, T.; Kami, K.; Arata, Y.; Shimada, I. *Nat. Struct. Biol.* **2000**, *7*, 220−223.
(45) Volke, F.; Eisenblätter, S.; Klose, G. *Biophys. J.* **1994**, *67*, 1882−1887.
(46) Ulrich, A. S.; Watts, A. *Biophys. J.* **1994**, *66*, 1441−1449.
(47) Seelig, A.; Seelig, J. *Biochemistry* **1974**, *13*, 4839.
(48) Palmer, L. R.; Merrill, A. R. *J. Biol. Chem.* **1994**, *269*, 4187−4193.
(49) Kienker, P. K.; Qiu, X.; Slatin, S. L.; Finkelstein, A.; Jakes, K. S. *J. Membr. Biol.* **1997**, *157*, 27−37.

penetrating the bilayer, thus providing an ideal model system for a surface-bound macromolecule. Spin diffusion from the lipid chain termini to DNA is largely a magnetization transfer process through the lipid bilayer.

Spin diffusion in pure lipids is extremely inefficient. Contrary to the rigid membrane protein, MAS averages the dipolar couplings in the lipid phase and yields highly resolved ^{1}H spectra even at relatively mild spinning speeds.[16] This is due to the rapid axially symmetric reorientation of the phospholipids about the bilayer normal, which converts the homogeneous ^{1}H−^{1}H dipolar interaction into an inhomogeneous broadening.[50] Therefore, magnetization transfer in lipids is a cross-relaxation phenomenon and is much less efficient than spin diffusion by nonaveraged dipolar couplings in rigid molecules.[51]

The cross-relaxation process in the lipid matrix has been analyzed in detail by Gawrisch and co-workers.[25,52] It was found that magnetization transfer is largely an intermolecular process between neighboring molecules. Only directly neighboring methylene groups exchange magnetization partially by intramolecular cross-relaxation. Even the cross-peak between lipid chain ends and headgroups is purely intermolecular and results from chain upturns that put these segments into direct contact.[52] Intramolecular magnetization transfer within the lipid chains is an even slower process that does not contribute to cross-peak intensities for mixing times on the order of a few hundred milliseconds. These results reflect the high mobility and structural heterogeneity of lipid molecules in bilayer membranes, which have also been observed in molecular dynamics simulations.[53]

The experimental methyl-to-DNA spin-diffusion curve does not reach a plateau even after 2.2 s, with a much smaller slope than that of colicin (Figure 8). This clearly shows that magnetization transfer through a lipid matrix without a rigid TM domain is inefficient. Importantly, this slow spin diffusion is true even after taking into account the intermolecular contacts due to chain upturns. The ^{1}H NOESY relaxation matrix analysis for the DOTAP/DNA sample (Figure 8) further confirms the slow magnetization transfer in the lipid phase. Thus, one can readily distinguish between proteins that have or lack a membrane-embedded domain.

In simulating the methyl-to-DNA build-up curve, a single lipid diffusion coefficient of 0.0012 nm^2/ms was used for the bilayer. This approximation neglects the fact that the ^{1}H−^{1}H dipolar couplings increase from the bilayer center toward the glycerol backbone. However, this unknown lipid diffusion coefficient does not change the conclusion about the geometry of the DNA/DOTAP complex, since the latter is already known from diffraction studies. While the use of a single phenomenological diffusion coefficient does not fully represent the complexity of the lipid bilayer, the purpose of the experiment is to demonstrate the drastic difference in spin diffusion due to the presence or absence of transmembrane segments in macromolecules. This difference is indeed observed empirically.

It is interesting to note that spin diffusion from water into DNA is somewhat slower as compared to spin diffusion from water to colicin (not shown). One would expect the water molecules to be sufficiently close to DNA to facilitate magnetization transfer. There are three possibilities for this observation. First, the DNA/DOTAP mixture is less hydrated than the colicin−lipid mixture. The distance between opposing bilayers, determined by the DNA diameter, is 20 Å, and the repeat spacing between neighboring DNA strands is only 26 Å.[30] Thus, the DNA/DOTAP system only contains about 15 wt % water as compared to the 30 wt % for the membrane-bound colicin. Similar dehydration was also reported in other polyelectrolyte/membrane systems.[54,55] Second, DNA is more mobile than colicin. The typical order parameters of the backbone of membrane-bound colicin are around 0.9,[21] while the order parameter of the DNA phosphate is 0.82 based on the static ^{31}P line shape. Therefore, ^{1}H−^{1}H dipolar couplings near the DNA phosphates are reduced, reducing spin-diffusion rates. Finally, the average ^{1}H density in DNA is about 20 times lower than that in helical proteins. The longer ^{1}H−^{1}H distances further reduce the ^{1}H−^{1}H dipolar couplings responsible for magnetization transfer.

^{31}P-Detected Spin Diffusion via Transmembrane Protein Segments. Qualitative information about membrane protein topology can be obtained indirectly by detecting the lipid ^{31}P signal. The rigid TM segments expedite the usually slow magnetization transfer from the chain termini to the headgroups. The magnetization pathway starts from the acyl chain ends, continues via the transmembrane protein, and finally reaches the lipid phosphate groups. In this way, methyl-to-phosphate spin diffusion is much faster with a TM domain than without. The ^{31}P-detected spin-diffusion curve is slightly shallower than the Ala Cα-detected curve. This is because two rate-limiting interface transfer steps, from the methyl to the protein, and from the protein to the lipid, are now present, one more than in the ^{13}C-detected experiment.

The ^{31}P-detected experiment requires no isotopic labeling of the protein and no high-power ^{1}H decoupling. Thus, it can be performed on a solution NMR spectrometer with a high-resolution MAS probe. Further, ^{31}P is a higher-sensitivity nucleus than ^{13}C, making it possible to collect a complete set of spin-diffusion data in a relatively short time.

The present lipid-initiated ^{1}H spin-diffusion experiment is best suited for large membrane proteins where global topology information is desired. It is less applicable to small peptides, since their typical mobility reduces the ^{1}H diffusion coefficient to be comparable to that of the lipid. This would make the spin-diffusion build-up much less different between a transmembrane peptide and a surface-bound peptide.

Conclusions

We have shown that a simple 2-D ^{1}H spin-diffusion experiment initiating the magnetization transfer from the methyl protons at the lipid chain termini provides useful topological information about membrane proteins. The slope of the spin-diffusion build-up curves determines unambiguously the presence or absence of membrane-embedded domains in the protein, which is difficult to obtain otherwise for a complex protein containing multiple domains. Proteins with transmembrane domains have much faster magnetization transfer than surface-

(50) Davis, J. H.; Auger, M.; Hodges, R. S. *Biophys. J.* **1995**, *69*, 1917−1932.
(51) Edzes, H. T.; Samulski, E. T. *J. Magn. Reson.* **1978**, *31*, 207−229.
(52) Huster, D.; Gawrisch, K. *J. Am. Chem. Soc.* **1999**, *121*, 1992−1993.
(53) Feller, S. E.; Huster, D.; Gawrisch, K. *J. Am. Chem. Soc.* **1999**, *121*, 8903−8904.
(54) Steffan, G.; Wulff, S.; Galla, H. J. *Chem. Phys. Lipids* **1994**, *74*, 141−150.
(55) Huster, D.; Dietrich, U.; Gutbherlet, T.; Gawrisch, K.; Arnold, K. *Langmuir* **2000**, *16*, 9225−9232.

bound molecules such as DNA. The maximum depth of insertion of the membrane-embedded domains can be estimated from numerical simulations of the build-up curves. Also, comparisons between the spin diffusion from water and from the lipid chains provide information on the relative fraction of membrane-embedded and surface-associated residues in the protein. The experiment utilizes heteronuclear detection, which can be ^{13}C and ^{15}N for proteins and ^{31}P for DNA. The enhanced ^{1}H spin diffusion due to rigid transmembrane protein segments can also be detected through the lipid ^{31}P resonance, thus removing the need for isotopic labeling of the protein. This lipid-initiated spin-diffusion experiment is simple, can be performed on multilamellar membrane preparations, and requires only standard NMR hardware under MAS.

Acknowledgment. M.H. thanks the Arnold and Mabel Beckman Foundation for a Young Investigator Award and the National Science Foundation for a CAREER award (MCB-0093398). D.H. is grateful for a postdoctoral fellowship from the BASF AG and the Studienstiftung des deutschen Volkes.

JA017001R